Synthesis, growth, Spectral, third order nonlinear optical and antimicrobial behaviour of 5-bromopyridine-4-hydroxybenzoic acid single crystals

B. MOHANBABU[a], R. BHARATHIKANNAN[b*], G. SIVA[b]
[a]Departmet of Physics, Sri Shakthi Institute of Engineering and Technology, Coimbatore
[b]Departmet of Physics, SRMV College of Arts and Science, Coimbatore

The slow evaporation technique was adopted for the growth of single crystals of 5-bromopyridine-4-hydroxybenzoic acid at room temperature. At the beginning of the process of analysis, the crystal was subjected to single crystal X-ray diffraction analysis. The Mulliken atomic charge and the values of electronegativity and chemical hardness index were calculated to interpret and predict the reactive behaviour. Due course, frontier molecular orbitals energies were analysed to explain the eventual charge transfer interactions that takes place within the molecules. Further, the dielectric study highlighted thatthe low dielectric constant value was observed at a high frequency range. The stiffness constant and yield strength were also calculated by the micro-hardness value. The total static dipole moment (μ), mean polarizability (α), anisotropy of polarizability ($\Delta\alpha$) and first order hyperpolarizability (β) were calculated from Gaussian output. Finally, the third order nonlinear optical parameters like refractive index (n2), absorption coefficient (β) and third order susceptibility ($\chi^{(3)}$) were estimated by Z-scan studies. The compound exhibited a good antibacterial and antifungal activity compared with standard antibacterial and fungal species. The compound has significant antioxidant activity against free DPPH radicals.

1. Introduction

Recent interest in quantum electronics has centred on "finding the new materials for efficient second-harmonic generators, tunable parametric oscillators and broadband electro optic modulators. Many organic materials have been found to have greatly nonlinear or optoelectrical properties than inorganic substances" [1-3]. Efforts have been made on the mixed organic and inorganic complex crystals in order to make them suitable for device applications such as optical switches, optical modulators, optical bistable devices, electro optical devices, etc. Inorganic NLO crystals have usually a high melting point, high mechanical strength and high degree of chemical inertness. The nonlinearity of these materials is low when compared to organic NLO crystals. The applications of organic NLO crystals have developed rather slowly because the organic molecules are constructed by van der waal and hydrogen bonds, and it is difficult to grow large, optical- quality single crystals and also, due to the often fragile nature of these crystals [4,5]. It is also difficult to cut and polish the crystals. In order to overcome these difficulties ''semi-organic'' materials have been proposed as a new approach for materials with interesting nonlinear optical properties. In last several years, the search is focused on new types of NLO materials which combines the advantages of organic and inorganicmaterials called semi-organic materials. Two types of semi organic

material include organic and inorganic salts and metal organic coordination complexes [6].

Moreover, Pyridine derivatives are prominent materials in the field of biology as they show a wide range of biological properties like antitumor, antibiotics, psychotropic, anti-inflammatory, and antihistaminic activities. This pyridine moiety presences in many large complexes repeatedly with fascinating applications in catalytic, photophysical, and electrochemical field [7, 8]. Hence, they have been expected as useful drugs for the treatment of many diseases like myocardial infarction and diarrhea. This has led to the development of new drugs based on pyridine. Because of the above mentioned properties and applications, we study the crystalline perfection and other physical properties of the pyridine based materials. In the presence of nitrogen atom in pyridine ring, the chemical is used as an efficient material for the establishment of charge transfer molecule.

In this research work, the single crystals of 5-bromopyridine-4-hydroxybenzoic acid (BPHB) were grown by slow evaporation solution growth technique in room temperature. The grown crystals were subjected for the various characterization such as Single X-ray diffraction analysis, UV–vis spectroscopy, dielectric study, and hardness studies. The third order nonlinear optical parameters like refractive index, absorption coefficient and susceptibility were calculated for the grown crystals. Furthermore, quantum chemical density functional calculations including Mulliken atomic charges, frontier

molecular orbitals, thermal properties and hyperpolarizability have been calculated for the BPHB crystal. The antibacterial and antifungal activities of the synthesized complex were examined against various bacteria and fungi species. The compound is subjected to the antioxidant activity against free DPPH radicals.

2. Experimental

Material synthesis

For the preparation of charge transfer complex of 5-bromopyridine-4-hydroxybenzoic acid (BPHB), AnalaR grade samples of 5-bromopyridine and 4-hydroxybenzoic acid were employed for the synthesis of the title compound. Methanolic solutions of the two reactants were prepared separately in 1:1 molar ratio and mixed together. The resulting solution was stirred well for an hour. The precipitated material was filtered off and repeatedly recrystallized from methanol to enhance the degree of purity of the synthesized compound.

Solubility

Growth of the crystals with well-defined morphology depends mainly on the solvent which is used for crystal growth. Solvents offering moderate solubility-temperature gradient for a material and yielding prismatic growth habit will be chosen for growing single crystals of that material. For choosing the most suitable solvent for crystal growth, valuable information can be obtained through solubility test [9]. The different solvents were used to find suitable solvents for BPHB crystal. The solvents methanol and chloroform were used. The solubility was measured for different temperatures (30–45°C) for methanol and chloroform respectively. It was observed that BPHB exhibits the high positive solubility temperature gradient in methanol solvent than in chloroform. Hence methanol has been chosen as the solvent for crystal growth. The solubility curves are shown in Figure 1.
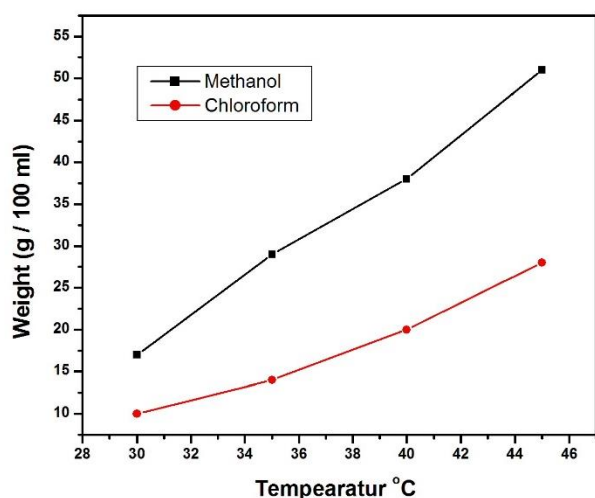

Fig.1. The Solubility diagram of BPHB crystal

Single crystal growth

A saturated solution of the title compound in methanol was prepared, stirred well for about an hour and heated slightly to dissolve the undissolved particles. Then the solution was filtered through a whatmann 41 grade filter paper to remove the suspended impurities. The clear filtrate was collected in a 250ml beaker and kept unperturbed in a dust free room for the growth of single crystals of the compound. Well defined brown coloured single crystals were harvested at the end of the seventh day.

Material Characterisation

The X-Ray diffraction intensities were measured on a Bruker Smart X2S diffractometer at 296K. The well-collimated Mo Kα radiation (λ = 0.71073 Å) and the ω-scan mode were employed. The UV-visible absorption and transmittance spectra were recorded on SYSTRONICS DOUBLE BEAM UV-Vis spectrophotometer operating between 200 and 800 nm. Dielectric studies were carried out using HIOKI multifrequency LCR meter. Mechanical properties of the grown crystal were studied using a Vicker's micro-hardness tester with a diamond pyramidal indenter. The single beam Z-Scan technique was used to determine the magnitude and higher order nonlinearity of the grown crystal. The Nonlinear refractive index (n_2) and nonlinear absorption coefficient (β) were investigated.

Computational details

Quantum chemical calculations of the title compound were carried out with Gaussian03 software program [10] and the Gauss View molecular visualization program [10]. Mulliken atomic charges, Frontier Molecular Orbitals and Thermodynamic Properties values were calculated for the BPHB crystal by using B3LYP (Becke's three-parameter hybrid model using the Lee-Yang Parr correlation functional) methods which consist of the Lee–Yang–Parr correlation functional in conjunction with a hybrid exchange functional first proposed by Becke [11,12]. The Donor and the acceptor occupancy and of the stabilization energy of the different overlapping for the title compound was studied by using B3LYP/6-311++G basis set. Furthermore, the dipole moment (μ), the polarizability (α) and the first-order hyperpolarizability (β) of the title compound under study were calculated by B3LYP/6-311++G level.
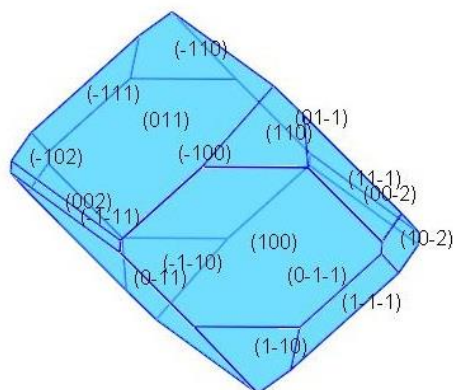

Fig.2. The ORTEP diagram of BPHB crystal

Antibacterial activity

The antibacterial activity of newly synthesized title compound was tested against Staphylococcus aureus, Bacillus substilis, Klebsiella pneumonia, and Pseudomonas aeruginosa by Kirby–Bauer method [13]. Media with DMSO solvent was set up as control. The discs measuring 5 mm in diameter were prepared from Whatman No. 1 filter paper sterilized by dry heat at 140 o C for 1 h. The sterile discs previously soaked in a concentration of the test compounds were placed in a nutrient agar medium. The petri plates were invested and kept in an incubator for the time period of 24 h at the temperature of 37o C and growth was monitored visually. The screening was performed at 100 lg/mL concentration of test complexes and antibiotic disc. Ciprofloxacin (10µg/disc) was used as control. Logarithmic serially two fold diluted amount of test complexes and controls was inoculated within the range 104–105 cfu/mL. To obtain the diameter of zone, 0.1 ml volume was taken each and spread on agar plates. The number of colony forming units (cfu) was counted after 24 h of incubation at 35° C. After incubation the zone of inhibition was measured and expressed as mm in diameter [14, 15].

Antifungal activity

The newly synthesized compound was also screened for its antifungal property against Aspergillus niger, Aspergillus flavus, Aspergillus fumigatus and Penicillium sp. in DMSO solvent by using standard agar disc diffusion method. The synthesized compound was dissolved in DMSO as a solvent and media with DMSO was set up as a control. All cultures were routinely maintained on Sabouraud Dextrose Agar (SDA) and incubated at 28 °C. Spore formation of filamentous fungi was formed from seven days old culture on sterile normal solution, which was diluted to approximately 105 cfu/mL and the culture was centrifuged at 1000 rpm. The pellets were resuspended and diluted in sterile Normal Saline Solution (NSS) to obtain a viable count 105 cfu/mL. With the help of spreader, 0.1 mL of approximately diluted fungal culture suspension was spreaded on agar plates. The fungal activity of compound was compared with clotrimazole (10 µg /disc) which is used as a standard drug. The cultures were incubated for 48 h at 37 ºC and the growth was monitored. Antifungal activity was determined by measuring the diameters of the zone (mm) in triplicate sets.

Antioxidant activity

DPPH radical scavenging activity of extract was determine according to the method reported by Blois [16]. An aliquot of 0.5 ml of sample solution in methanol was mixed with 2.5 ml of 0.5 mM methanolic solution of DPPH. The mixture was shaken vigorously and incubated for 30 min in the dark at room temperature. The absorbance was measured at 517 nm using UV spectrophotometer. Ascorbic acid was used as a positive control. DPPH free radical scavenging ability (%) was calculated by using the formula. % of inhibition = absorbance of control – absorbance of sample / absorbance of control ×100. The ascorbic acid was used as standard molecule for comparison of the tested sample. The principle in this method is that the antioxidants (synthesized compound) react with the stable DPPH free radical (deep violet colour) and convert it to 2, 2-diphenyl-1-picrylhydrazine with decolourisation. The degree of decolourisation shows the scavenging ability of the antioxidant compound.

3. Result and discussion

Single crystal XRD analysis

Good quality crystal of BPHB was subjected to X-ray diffraction analysis. The single crystal structure determination of BPHB has been carried out at room temperature using Brukeraxs (Kappa apex2) diffractometer at 293 K using Mo Kα radiation (λ = 0.71073 Å). For X-ray data collection, a single crystal of size 0.18 x 0.16 x 0.12 mm^3 was used. The unit cell parameters were obtained by using many high angle reflections. The structure was solved by using SHELXS 97 (Sheldrick 1997) and refined by full-matrix least-squares refinement method using SHELXL 97 (Sheldrick 1997) program. The intensity data were collected for h from -7 to 7, for k from -18 to 17 and for l from -19 to 18. The compound crystallizes in the monoclinic system with space group of P21/c. The unit cell parameters for the crystal are a = 5.900(5), b = 13.776(5), c = 14.438(5), α = 90.000(3) deg, β = 97.543(5) deg. And γ = 90.000(4) deg. The ORTEP of the molecule with displacement ellipsoids at 50% probability level are given in figure 3.
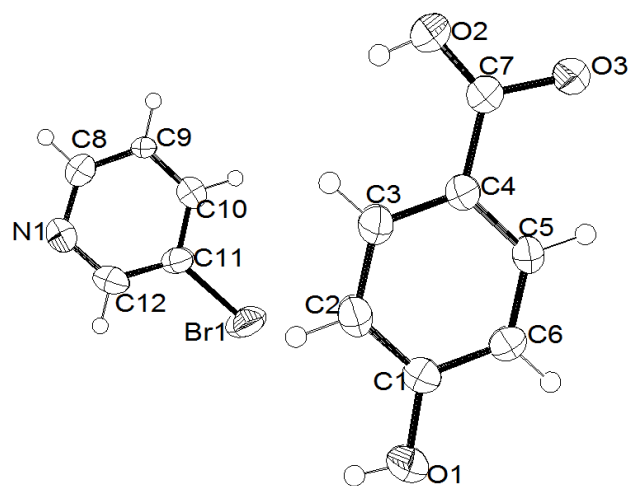

Fig.3 . The packing diagram of BPHB crystal

The packing of the molecules in the unit cell is shown in figure 4. The crystal structure data are presented in table 1. The stacking of 5-bromopyridine and 4-hydroxy benzoic acid as alternate layers is seen in the packing diagram. The stacking shows a strong interaction existing between 5-bromopyridine and 4-hydroxy benzoic acid moieties.
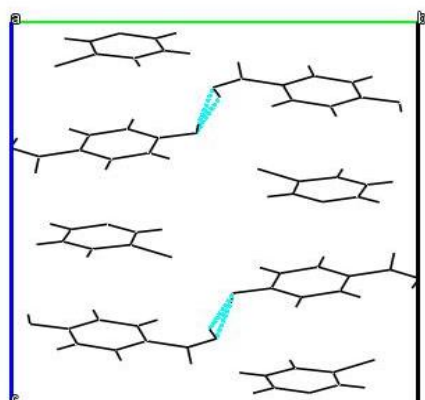
Fig.4. The morphology of the BPHB crystal

Mulliken Atomic Charge

Mulliken atomic charge calculation has played a chief role in the application of quantum chemical calculation to molecular system. The dipole moment, molecular polarizability, electronic structure and a lot of properties of molecular systems are depend on atomic charges. The charge distributions over the atoms advocate the formation of donor and acceptor pairs which involves the charge transfer in the molecule. The calculated Mulliken charge distribution structure of BPHB crystal is shown in Figure 5. The oxygen and nitrogen atoms have more negative charges whereas all hydrogen atoms have a positive charge. Moreover, Mulliken atomic charges also shows that the bromine atom in the 5-bromopyridine moiety ring has positive atomic charge (0.134825 e). The variations in atomic charges of hydrogen atoms are formed by the establishment of hydrogen bonding. However, the sum of Mulliken atomic charges of all atoms of BPHB molecule maintains the charge neutrality. Mulliken population analysis is a good way to account for differences in electro negativities of atoms within the molecule Mulliken population method can be used for interpreting and predicting the reactive behaviour of a wide variety of chemical systems in both electrophilic and nucleophilic reactions.
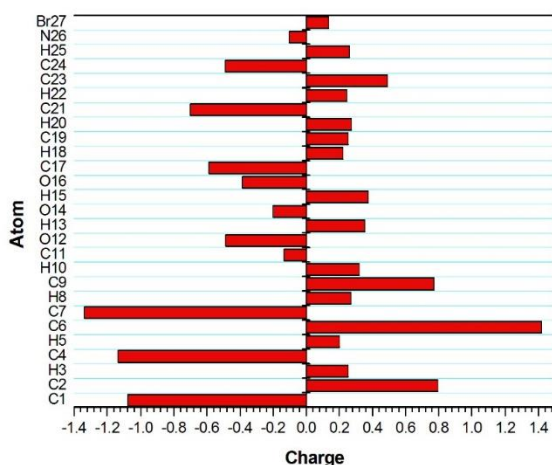

Fig.5. The mulliken atomic charges of BPHB crystal

Table 1 - Crystal data and structure refinement for BPHB

Identification code	shelxl
Empirical formula	C12 H10 Br N O3
Formula weight	296.12
Temperature	293(2) K
Wavelength	0.71073 Å
Crystal system, space group	MONOCLINIC, P21/c
Unit cell dimensions	a = 5.900(5) A alpha = 90.000(5) deg.
	b = 13.776(5) A beta = 97.543(5) deg.
	c = 14.438(5) A gamma = 90.000(5)deg.
Volume	1163.3(11) A^3
Z, Calculated density	4, 1.685 Mg/m^3
Absorption coefficient	3.528 mm^-1
F(000)	588
Crystal size	0.18 x 0.16 x 0.12 mm^3
Theta range for data collection	2.05 to 28.44 deg.
Limiting indices	-7<=h<=7, -18<=k<=17, -19<=l<=18
Reflections collected / unique	11041 / 2886 [R(int) = 0.0354]
Completeness to theta	28.44 98.6 %
Absorption correction	Semi-empirical from equivalents
Max. and min. transmission	0.7192 and 0.5388
Refinement method	Full-matrix least-squares on F^2
Data / restraints / parameters	2886 / 0 / 156
Goodness-of-fit on F^2	1.035
Final R indices [I>2sigma(I)]	R1 = 0.0544, wR2 = 0.1369
R indices (all data)	R1 = 0.0795, wR2 = 0.1525
Extinction coefficient	0.0015(8)
Largest diff. peak and hole	1.610 and -1.075 e.A^-3

Analysis of Frontier Molecular Orbitals

The highest occupied molecular orbitals (HOMOs) and the lowest-lying unoccupied molecular orbitals (LUMOs) are named as Frontier Molecular Orbitals (FMOs) because they lie at the outermost boundaries of the electrons of compound. The frontier orbital gap helps characterize the chemical reactivity and the kinetic stability of the molecule. A molecule with a small frontier orbital gap is termed as soft molecule and is generally associated with high chemical reactivity and low kinetic stability [17]. In addition, the FMOs are important in determining the ability of a molecule to absorb light. The FMOs play an important role in the optical and electric properties, as well as in quantum chemistry and UV–vis spectra. HOMO, LUMO energy characterizes the ability of electron accepting. In dealing with interacting molecular

orbitals, the two that interact are generally the highest energy occupied molecular orbital (HOMO) and lowest unoccupied molecular orbital (LUMO) of the compound. These orbitals are a pair of orbitals in the compound, which allows them to interact more strongly. In order to evaluate the energetic behaviour of the title compound, the calculation were carried out in gas phase. The calculated energy values of HOMO and LUMO in gas phase are -0.2527 eV and -0.06655 eV, respectively, and the frontier orbital energy gap value is 0.18615 eV. HOMO and LUMO energies and surfaces can be seen in Figure 6. The narrow energy gap between HOMO and LUMO facilitates intramolecular charge transfer which makes the material to be NLO active.
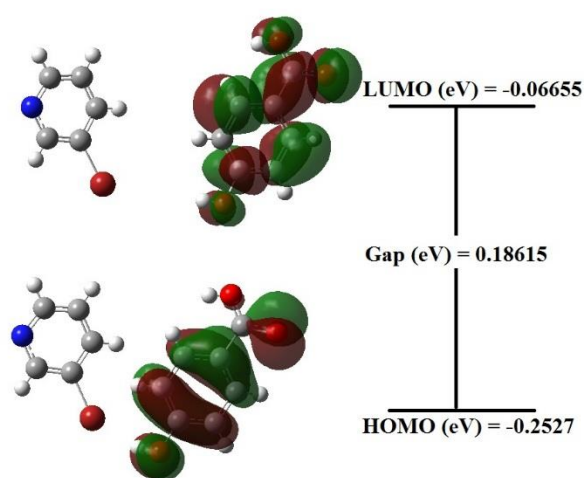

Fig.6. The distributions and energy levels of HOMO and LUMO orbitals for BPHB

Moreover, the energy band gap value helps us to identify the chemical reactivity and kinetic stability of a molecule. A small band gap energy of the molecule is generally related to high chemical reactivity and low kinetic stability. The ionisation energy (I) and electron affinity (A) are of great importance in the determination of biochemical pathways for electron transfer, photosynthesis, oxidative phosphorylation, and oxidative stress. The Ionisation energy is directly proportional to the electrochemical oxidation potentials of the compounds. The electron affinity gives an idea about the stability of free radicals and anions. The ionisation energy and electron affinity can be expressed through HOMO and LUMO orbital energies by Koopmans' theorem [18] as, $I = -E_{HOMO}$ and $A = -E_{LUMO}$. From the value of ionization energy and electron affinity, Mulliken electronegativity (χ) can be calculated from the equation $\chi = (I+A)/2$. The chemical potential (μ) is the negative value of the electronegativity. Softness (S) is a property of the molecule that measures the extent of chemical reactivity. It is the reciprocal of hardness ($S = 1/2\eta$). The hardness is calculated using the expression $\eta = (I-A)/2$ [19]. Parr et al., have proposed the global electrophilicity power of a system as, $\omega = \mu^2/2\eta$ [20]. This index measures the

stabilisation in energy when the system acquires an additional electronic charge from the environment. The values of electronegativity, chemical potential, chemical hardness, softness, and electrophilicity index of the title molecule are 0.15963 eV, -3.9809 eV, 0.09308 eV, 5.372 eV, and 0.13688 eV in gas phase, respectively.
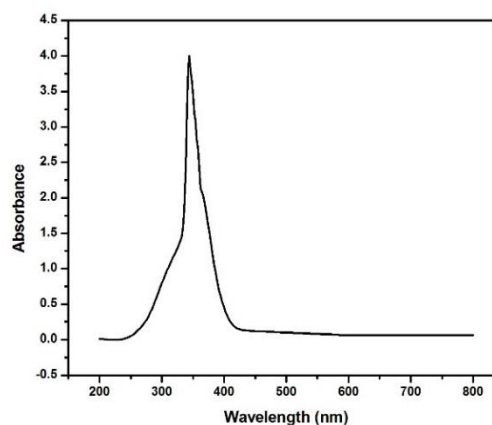

Fig.7. The UV absorption spectrum of the BPHB crystal

UV- visible spectral analysis

The linear optical characteristics of the grown crystal BPHB was studied with the help of SYSTRONICS DOUBLE BEAM UV-Vis spectrophotometer in the range 200 – 800 nm. The UV – visible absorption spectrum of the title compound is shown in the Figure 7. The absorption of UV and visible light involves the promotion of the electron in σ and π orbitals from the ground state to higher energy states in the molecule. The transition of electron in the grown crystal is occurred around 340 nm range. The longer wavelength absorption band arising due to the promotion of an electron from the highest occupied molecular orbital to the lowest unoccupied molecular orbital which confirms the formation of charge transfer in molecular complex. The transmittance spectrum of the BPHB crystal is depicted in the figure 8. From the spectrum, it is clear that UV cut-off wavelength of grown crystal is noted at 400 nm. The crystal is entirely transparent beyond cut-off wavelength up to 800 nm. The cracking and blackening impurities directly affect the optical transmittance. But no distortion was observed in the transmittance spectrum of the grown crystal. Hence, this illustrates the suitability of the crystal for second and third harmonic generation of wavelength [21, 22].

The optical absorption co-efficient (α) of grown crystal was obtained from the following relation,

$$\alpha = \frac{2.303 \log (1/T)}{d}$$

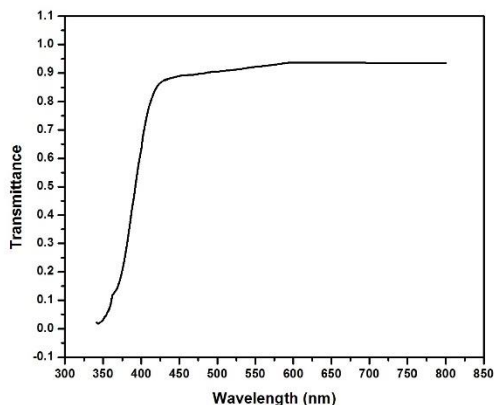Where, d is the thickness of the crystal and T is the transmittance.

Fig.8. The UV transmittance spectrum of the BPHB crystal

Owing to the allowable indirect band gap, the crystal under study has an absorption coefficient (α) obeying the following relation for high photon energies ($h\upsilon$): $(\alpha h\upsilon) = A (h\upsilon - E_g)^n$. Where A is constant, 'h' is Planck's constant and υ is frequency of incident photons. The optical energy gap [E_g] of BPHB is calculated by using the plot of $h\upsilon$ versus $(\alpha h\upsilon)^{1/n}$, by extrapolating the linear portion of the curve near the start of absorption edge towards the energy axis [23] is shown in figure 9. The band gap value of the grown crystal was found as 2.86 eV. This wide band gap of this crystal shows the large transmittance of visible region.
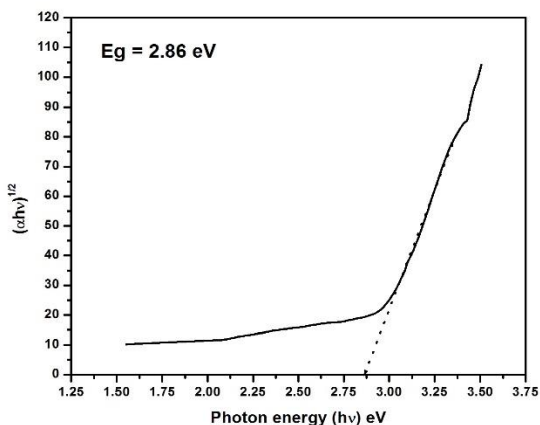

Fig.9 . The plot of $h\upsilon$ versus $(\alpha h\upsilon)^{1/2}$ for BPHB crystal

The optical band gap and extinction coefficient are most important to examine the material's optoelectronic applications [24]. The optical constants are determined from the transmission (T) and reflection (R) spectrum based on the following relations [25].

$$T = \frac{(1-R)^2 \exp(-\alpha t)}{1 - R^2 \exp(-2\alpha t)}$$

Where t is the thickness and α is absorption coefficient.

The reflectance (R) in terms of the absorption coefficient and refractive index (n) can be derived from the following relations:

$$R = \frac{1 \pm \sqrt{(1-\exp(-\alpha t)+\exp(\alpha t))}}{1+\exp(-\alpha t)}$$

$$n = \frac{-(R+1) \pm \sqrt{(-3R^2 +10R-3)}}{2(R-1)}$$

Fig. 10 shows the energy dependence of refractive index (n) for the grown BPHB crystal. The refractive index of the material increases while increasing the photon energy. The refractive index (n) for BPHB crystal is 0.4505 at wavelength of 632 nm.
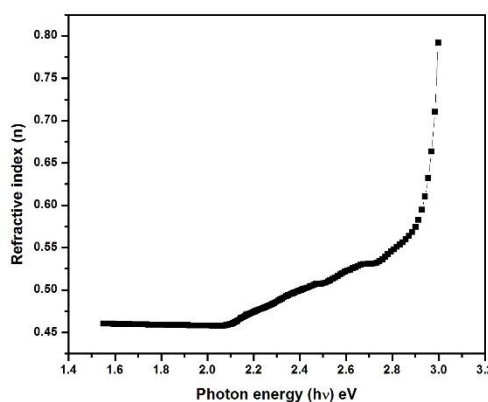

Fig.10. The energy dependence of refractive index (n) for BPHB crystal

Dielectric study

The study of the dielectric properties of the crystal gives information about the electric field distribution within the solid. The frequency dependence of these properties gives an idea about the material's applications. The different polarization mechanisms in the crystal can be understood from the study of dielectric constant as a function of frequency and temperature. To study the dielectric response of the grown crystal, the two opposite surfaces across the breadth of the sample were treated with good quality silver paste in order to obtain good ohmic contact. The capacitance of the crystal is measured for the frequency range of 50Hz-200 kHz at various temperatures. The Figure 11 shows the plot of dielectric constant (ε_r) between frequencies for the various temperature ranges of 28°C, 33°C, 38°C and 43°C is shown in. The dielectric constant of the crystal is calculated using the relation $\varepsilon_r = C_{crys}d/\varepsilon_0 A$, where C_{crys} is the capacitance of the crystal, d is the thickness of the sample, ε_0 is the permittivity of free space and A is the area of the sample used. In the lower frequency region, the dielectric constant has the higher values. Further, the dielectric constant starts to decrease with increasing the frequency. The presence of space charge, orientation, electronic, and ionic polarizations contribute to the very high values of dielectric constant at low frequencies. Nevertheless, the loss of significance of these polarizations gradually is the

reason for the low value of dielectric constant at a higher frequencies. The defects have no long enough time to rearrange in response to the applied voltage at higher frequency. Hence the capacitance of the sample decreases with the increasing frequency [26]. According to the Miller rule, the lower value of dielectric constant at higher frequencies has a suitable parameter for the enhancement of SHG coefficient [27]. The Figure 12 shows the function of dielectric loss with log frequency. The low dielectric loss at high frequencies range suggests that the grown crystal possesses optical quality with lesser defects. Henceforth, this approves the grown crystal may be useful in the fabrication of nonlinear optical devices [28].
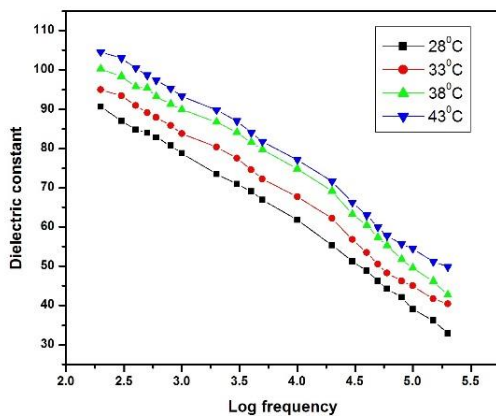

Fig.11 . The plot of dielectric constant (ε_r) and frequencies of BPHB crystal.

Hardness studies

Hardness tests are normally carried out to determine the mechanical strength of materials and it correlates with other mechanical properties like elastic constants and yield stress. The hardness of the material is defined as the resistance offered by a material to localized plastic deformation caused by indentation. Besides, microhardness study is applied to understand the plasticity of the crystal, as the hardness properties are basically related to the crystal structure of the material and the bond strength. Leitz Vickers microhardness tester fitted with a Vickers diamond pyramidal indenter, which is attached to an incident light microscope, is used to study the hardness of the material. The static indentations were made at room temperature with a constant indentation time 10 s for all indentations. The indentation marks were made on the surfaces by varying the load from 25 to 200 g. As micro cracks were developed at higher loads, the maximum applied load was restricted to 200 g only. The Vickers microhardness number Hv of the crystal is calculated using the relation

$$H_V = \frac{1.8544P}{d^2}\,\text{kg/}\mu\text{m}^2$$

where P is the applied load and d the average diagonal length of the indented impressions in millimeter. Fig. 13 shows the Vickers microhardness profile as a function of the applied test loads. It is evident from the plot that the microhardness values of BPHB is in agreement with the normal indentation size effect.
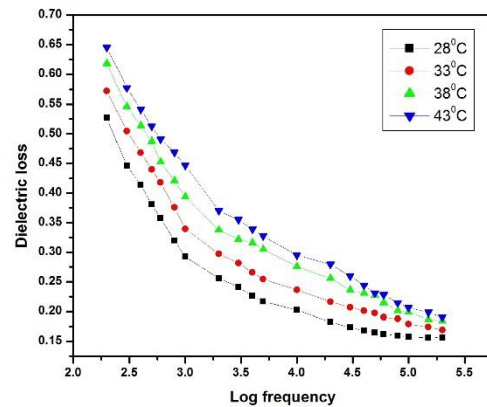

Fig.12. The function of dielectric loss with log frequency of BPHB crystal.
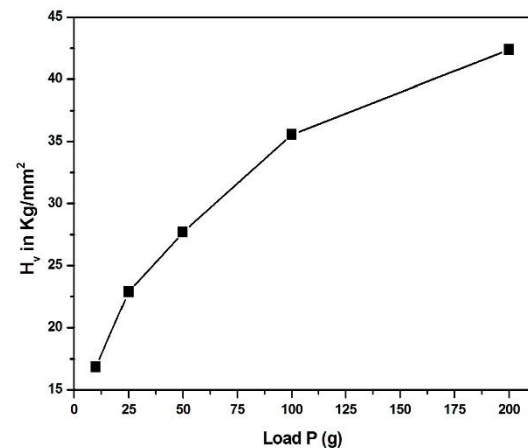

Fig.13. The Vickers microhardness profile as a function of the applied test loads.

The Meyer's index number was calculated from Meyer's law, which relates the load and indentation diagonal length and is given by P =kd^n, where k is the material constant and n is Meyer's index. The plot between log P and log d is shown in figure 14. The slope of the straight line plot gives the value of Meyer's index number and is calculated as 2.899. As per the Viker hardness rule, H$_V$ should increase with the rate of P if n>2 (reverse ISE) and decrease if n<2 (normal ISE). When n=2, the hardness is independent of the load applied and is given by Kick's law [29]. Then, the value agrees well with the experiment. According to Onitsch and Hanneman, Meyer's index number (n) should lie between 1 and 1.6 for harder materials and for softer materials n should be above 1.6 [30, 31]. Hence, BPHB belongs to the soft material category (n = 2.785). The stiffness constant (C11) gives

details about the nature of bonding between the neighbouring atoms. The stiffness constant is the property of the material by virtue of which it can absorb maximum energy before fracture occurs. The stiffness constant (C11) is calculated from Wooster's empirical relation given by $C11 = Hv^{7/4}$ [32].The variation of stiffness constant with various loads is illustrated in Fig. 15.
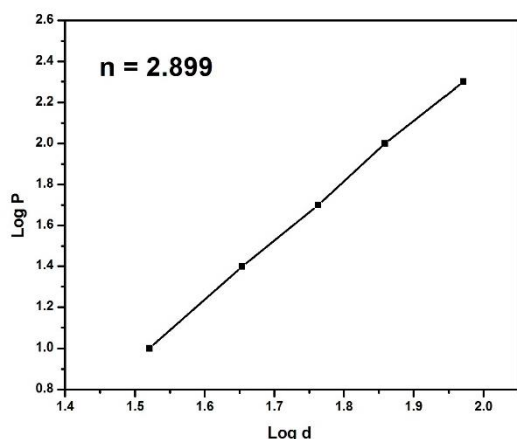

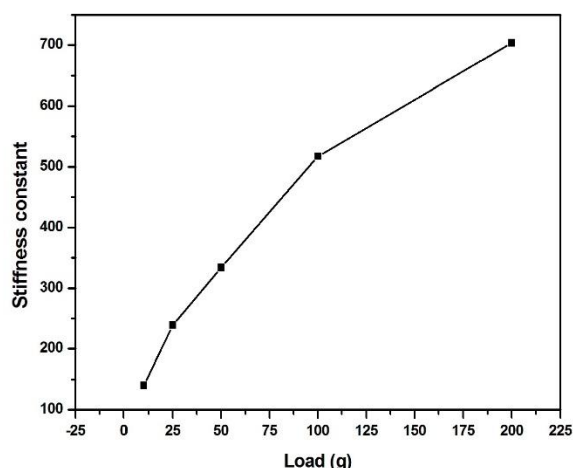
Fig.14. The plot between log P and log d of BPHB crystal.

Fig.15. The variation of stiffness constant of BPHB crystal.

From the hardness values, the yield strength (σ_y) of the grown crystal can be calculated. The yield strength is defined as the stress at which the material begins to deform plastically. The value of the yield strength depends on Meyer's index number n. For n>2, σ_y can be calculated using the expression

$$\sigma_v = \frac{3-n}{2.9}\left(\frac{12.5(n-2)}{3-n}\right)^{n-z} H_v$$

For n<2, the yield strength is calculated using the following relation

$$\sigma_v = \frac{H_v}{3}$$

It is understood from Fig. 16 that the yield strength also increases as load increases.
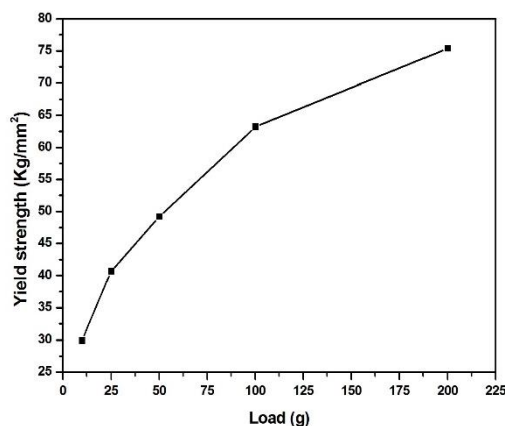

Fig.16. The variation of yield strength of BPHB crystal.

Thermodynamic properties

Thermodynamic properties of the BPHB crystals are calculated by using density functional methods with 6-311++G basis set. On the basis of vibrational analysis, the Zero Point Vibrational Energy, heat capacity, entropy and rotational constants of the title compound have been calculated from the theoretical harmonic frequencies.Several thermodynamic properties such as Zero Point Vibrational Energy (ZPVE), heat capacity (C_V), entropy (S) and rotational constants can be used to calculate the other thermodynamic energies and estimate the directions of chemical reactions according to relationships of thermodynamic functions and using second law of thermodynamics. The calculated thermodynamic properties are listed in Table 2. The BPHB molecule has Zero Point Vibrational Energy as 126.524 K Cal mol^{-1}, heat capacity as 40.770 Cal mol^{-1}K^{-1},entropy as 112.497 Cal/Mol-K and total thermal energy as 133.475 K Cal mol^{-1}. These thermodynamic data may provide useful information for the further study on the title compound.

Table 2 - Thermo dynamical parameter

Self-consistent field Energy (a.u.)		-3317.352
Zero point energy (Kcal/Mol)		126.52412
Rotational constant(GHZ)		0.39508
Rotational temperature (Kelvin)		0.01896
Energy (E) (KCal/Mol)	Translational	0.889
	Rotational	0.889
	Vibrational	131.698
	Total	133.475
Specific heat (C_v) (Cal/ Mol-Kelvin)	Translational	2.981
	Rotational	2.981
	Vibrational	34.809
	Total	40.770
Entropy(S) (Cal/ Mol-Kelvin)	Translational	42.943
	Rotational	36.858
	Vibrational	32.696
	Total	112.497
Dipole moment (Debye)		4.8727

Hyperpolarizability study

The interactions of electromagnetic fields in various materials produce the nonlinear optical (NLO) effects by altering the phase, frequency, amplitude or other propagation characteristics from the incident fields [33]. The hyperpolarizability and non-linear optical properties of an isolated molecule of potential NLO materials are considered as an extensive tool of research in molecular spectroscopy. To design the novel NLO materials, the theoretical investigation plays a key role in understanding the structure–property relationship. As the basis set of the density function calculation becomes larger, one can expect a better description of the compound and accordingly more accurate results. In the view of these points, B3LYP/6-311G++(d,p) method has been used to study the hyperpolarizability of the crystal. The complete equations for calculating the magnitude of the total static dipole moment (μ), mean polarizability (α), anisotropy of polarizability ($\Delta\alpha$) and first order hyperpolarizability (β) from Gaussian output are given below

$$\mu = \sqrt{\mu_x^2 + \mu}$$

$$\alpha = \frac{\alpha_x}{3}$$

$$\Delta\alpha$$

$$\alpha_{xx})^2 + 6\alpha_{xx}^2]^{1/2}$$

$$\beta = \left[(\beta_{xxx} + \beta_{xyy} + \beta_{xzz})^2 + (\beta_{yyy} + \beta_{yzz} + \beta_{yxx})^2 + (\beta_{zzz} + \right.$$

The polarizabilities and hyperpolarizability are reported in terms of atomic units (a.u) and the calculated values have been converted by using 1 a.u. = 0.1482 x 10^{-24} esu for α and 1 a.u. = 8.6393 x 10^{-33} cm5/esu for β. In the calculations, the values of the calculated dipole moment (μ), mean polarizability (α) and anisotropy of polarizability ($\Delta\alpha$) are 7.9602 Debye, 0.448 Å esu, 2.93 Å esu. The calculated first hyperpolarizability value (β) which is an important key factors for NLO properties of molecular system is equal to 1.0313 x 10^{-31} cm^5 esu^{-1}. In NLO studies, the urea is used as reference and its calculated values of μ, α, $\Delta\alpha$ and β are found to be 4.303 Debye, 1.39 Å esu, 0.934 Å esu, 0.563 x 10^{-31} cm^5 esu^{-1} respectively. In comparison with urea, the hyperpolarizability value of BPHB is almost equal to the two times that of urea.

Z-scan study

The magnitude and sign of nonlinear refraction (n_2) and nonlinear absorption coefficient (β) are measured simultaneously in the standard technique i.e. Z-scan technique [34]. The study of nonlinear refraction by the Z-scan method depends on the position (Z) of the thin sample under the investigation along with a focused Gaussian laser beam. The sample causes an additional focusing and defocusing, depending on whether nonlinear

refraction is positive or negative. The valley followed by a peak in the transmittance curve which is the signature for positive nonlinearity and it is known as the self-focussing effect. This is due to the local variation of refractive index with temperature. The data are expected to be symmetric with respect to focus, as a typical Z-scan data in open aperture mode is unresponsive to nonlinear refraction. For materials with multi-photon absorption, there is a minimum transmittance in focus (valley). There is a maximum transmittance in the focus (peak) for saturable absorber samples. Multi-photon absorption subdues the peak and augments the valley [35].

Fig. 17 and 18 show the measurements of open and closed aperture of the normalized transmittance (T). The open aperture of the normalized transmittance curve confirms that the crystal possesses themulti-photon absorption property. The nonlinear refractive index (n_2), nonlinear absorption coefficient (β) and third order susceptibility $\chi^{(3)}$ are calculated from the normalized transmittance curve [36, 37] for the BPHB crystals.
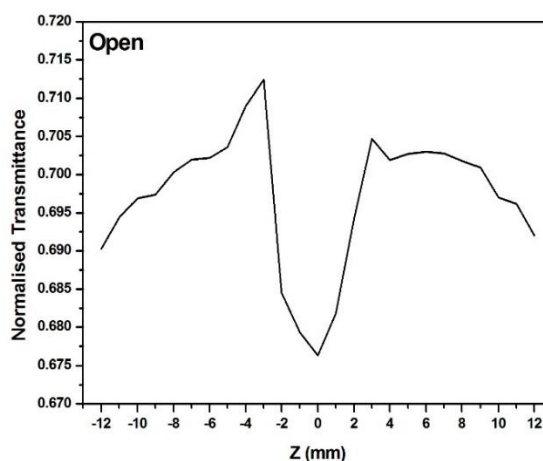

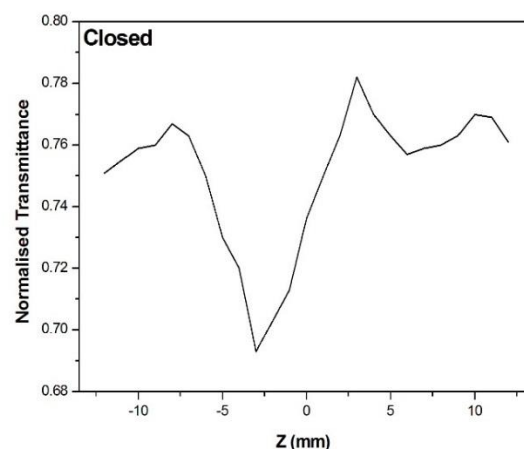*Fig.17. Measurements of open aperture of the normalized transmittance.*

Fig.18. Measurements of closed aperture of the normalized transmittance.

The nonlinear refractive index (n_2) is evaluated by the following relation,

$$n_2 = \frac{\Delta T_{p-v}}{0.406\,(1-s)^{0.25}\,kL_{eff}\,I_o}$$

where, ΔT_{p-v} is the difference between peak and valley transmittance, S is the linear aperture transmittance, k is the wave factor, $L_{eff} = \frac{1-e^{(-\alpha L)}}{\alpha}$ is the effective thickness of the sample and I_o is the on-axis irradiation at the focus (Z=0).

From the open aperture curve nonlinear optical absorption coefficient (β) was evaluated

$$\beta = \frac{2\sqrt{2}\,\Delta T}{I_0 L_{eff}}$$

The real and imaginary parts of the third order nonlinear optical susceptibility were determined by the following relations

$$Re\chi^{(3)} = 10^{-4}\frac{(\varepsilon_o C^2 n_0^2 n^2)}{\pi}\,(esu)$$

$$Im\chi^{(3)} = 10^{-2}\frac{(\varepsilon_o C^2 n_0^2 \lambda\beta)}{4\pi^2}\,(esu)$$

where ε_o the vacuum permittivity C is the velocity of light in vacuum. The absolute value of $\chi^{(3)}$ was obtained from the following relation

$$|\chi^{(3)}| = [(Re\chi^{(3)})^2 + (Im\chi^{(3)})^2]^{\frac{1}{2}}$$

The estimated nonlinear refractive index (n_2), nonlinear absorption coefficient and third order susceptibility values of BPHB are 0.888×10^{-8} cm^2/W and 3.394×10^{-5} cm/W and 2.349×10^{-8} esu. This indicates that the material reveals a positive refractive index, it results in the self-focusing nature and exhibits the third order nonlinearity. The open aperture data shows that the grown material possess the multi-photon absorption effect.

Antibacterial activity

In vitro, the bacteria species Staphylococcus aureus, Bacillus substilis, Klebsiella pneumonia, and Pseudomonas aeruginosa were prepared in the disc with the concentration of 100µg/disc. Ciprofloxacin was used as a standard drug to compare the activity results. The screening data of the sample and standard materials are given in Table 3. From the data, it is inferred that the cytotoxic activity is dose dependent. The synthesized compound shows good activity compare with standard drug. Among the number of bacterial species, the growth of Staphylococcus aureus was arrested to the larger amount than the other bacteria species. Nevertheless the synthesized compound molecule was active against the all bacterial species, it could reach the efficiency of standard drug to control the growth of bacteria. The result shows that the compound has potency for antibacterial activity.

Antifungal activity

The synthesized BPHB compound was also analysed for its antifungal activity using Clotrimazole as a standard drug for comparison of antifungal activity. The antifungal inhibition activity results of standard drug and synthesized compound are given in Table 4. The data confirms that the BPHB shows good inhibition activity against various fungal species. The BPHB compound also shows appreciable inhibition activity against Aspergillus niger. It is observed that the compound has the efficiency of antifungal activity.

Table 3 – Antibacterial activity of APHB Complex

S.No.	Organisms	Ciprofloxacin	BPHB
1.	Staphylococcus aureus	37	33
2.	Bacillus substilis	32	19
3.	Klebsiella pneumoniae	32	20
4.	Pseudomonas aeruginosa	36	31

Table 4 – Antifungal activity of APHB Complex

S.No.	Organisms	Clotrimazole	BPHB
1	Candida albicans	18	26
2	Aspergillus niger	27	22
3	Aspergillus fumigatus	25	26

Antioxidant activity

The DPPH method is simple, rapid and convenient method for scavenging of free radical. This method is widely used to examine the antioxidant properties of the compound. In the presence of compound, the stable DPPH radicals are capable of donating hydrogen atoms. Hence, the radical property is destroyed resulting in the colour change. The free radical scavenging ability of the synthesized compound with DPPH radical is studied in this analysis. The ascorbic acid was used as standard complex for comparison of results. The scavenging ability of the tested compound is represented in Figure 19. The result confirms that the synthesized compound can reduce the concentration of the initial free DPPH radicals. The IC 50 value of the BPHB compound is 271.6 µg/ml, whereas that for ascorbic acid is 101.6 µg/ml. This study confirms that the synthesized BPHB compound is capable of scavenging free radicals.
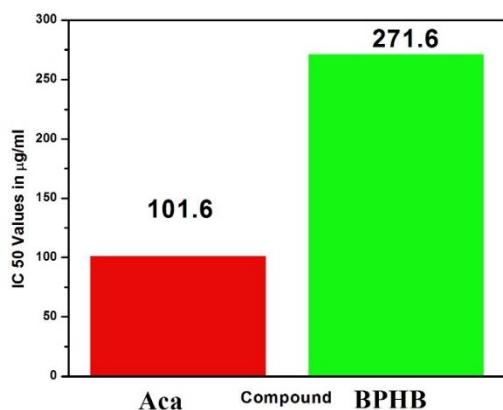
Fig.19. Antioxidant Activity of BPHB Compound

4. Conclusion

The 5-bromopyridine-4-hydroxybenzoic acid single crystals were synthesized and grown by adopting slow evaporation technique at ambient temperature. The centro-symmetry space group of the grown crystals were confirmed by the single crystal XRD analysis. UV-vis absorption analysis revealed that the electron transition took place around the wavelength of 340 nm. The transparency of the grown crystals was studied through UV-Vis transmission spectrum. The crystal showed the transparency beyond 400 nm wavelength (visible) region which is a desire property for various NLO applications. From the transmittance value, the optical band gap was calculated for the grown crystals as 2.86 eV. The characteristic of low dielectric loss at high frequencies for grown crystals suggests that the grown crystal possesses enhanced optical quality with lesser defects. The Vickers microhardness test revealed that the grown crystal was a soft material. The Mulliken atomic charge and Frontier Molecular Orbitals energy for the compound were determined. Thermodynamic properties and Hyperpolarisability values also have been calculated using density function methods. The Z-scan results reveals the self-focusing nature of the grown crystal. Besides, Antimicrobial studies reveal that the complex showed a good inhibition activity against a panel of bacterial and fungal species. The antioxidant activity confirmed that the charge transfer complex can serve as possible antioxidant against DPPH radical.

Reference

[1] J. Badan, R. Hierle, A. Perigaud, J. Zyss, ACS Symp. Ser. **233**, 81 (1983).

[2] D.S. Chemla, J. Zyss, Nonlinear Optical Properties of Organic Molecules and Crystals, Vols. 1, 2, Academic Press, New York, 1987.

[3] A.F. Garito, K.D. Singer, Laser Focus Fiberopt. Technol. **18**, 59 (1982).

[4] H.O. Marcy, M.J. Rosker, L.F. Warren, P.H. Cunningham, C.A. Thomas, L.A. Deloach, S. Pvelsko, C.A. Ebbers, J.H. Liao, M.G. Konatzidis, Opt. Lett. **20**, 252 (1995).

[5] T. Tsunekawa, T. Gotoh, and M. Iwamoto, Chem. Phys. Lett. **166**, 353 (1990).

[6] H.Q. Sun, D.R. Yuan, X.Q. Wang, X.F. Cheng, C.R. Gong, M. Zhou, H.Y. Xu, X.C. Wei, C.N. Luan, D.Y. Pan, Z.F. Li, X.Z. Shi, Cryst. Res. Technol. **40**, 882 (2005).

[7] A. Goel, V.J. Ram, Tetrahydron **65**, 7865 (2009).

[8] N.A. Al-Hashimy, Y.A. Hussein, Spectrochim. Acta, Part A **75**, 198 (2010).

[9] Holden, A.; Singer, P., Crystals and Crystal Growing, Doubleday and Company Inc, New York, 1960.

[10] M.J. Frisch, G.W. Trucks, H.B. Schlegel, G.E. Scuseria, M.A. Robb, J.R. Cheeseman, J.A. Montgomery Jr., T. Vreven, K.N. Kudin, J.C. Burant, J.M. Millam, S.S. Iyengar, J. Tomasi, V. Barone, B. Mennucci, M. Cossi, G. Scalmani, N. Rega, G.A. Petersson, H. Nakatsuji, M. Hada, M. Ehara, K. Toyota, R. Fukuda, J. Hasegawa, M. Ishida, T. Nakajima, Y. Honda, O. Kitao, H. Nakai, M. Klene, X. Li, J.E. Knox, H.P. Hratchian, J.B. Cross, C. Adamo, J. Jaramillo, R. Gomperts, R.E. Stratmann, O. Yazyev, A.J. Austin, R. Cammi, C. Pomelli, J.W. Ochterski, P.Y. Ayala, K. Morokuma, G.A. Voth, P. Salvador, J.J. Dannenberg, V.G. Zakrzewski, S. Dapprich, A.D. Daniels, M.C. Strain, O. Farkas, D.K. Malick, A.D. Rabuck, K. Raghavachari, J.B. Foresman, J.V. Ortiz, Q. Cui, A.G. Baboul, S. Clifford, J. Cioslowski, B.B. Stefanov, G. Liu, A. Liashenko, P. Piskorz, I. Komaromi, R.L. Martin, D.J. Fox, T. Keith, M.A. Al-Laham, C.Y. Peng, A. Nanayakkara, M. Challacombe, P.M.W. Gill, B. Johnson, W. Chen, M.W. Wong, C. Gonzalez, J.A. Pople, Gaussian 03, Revision D.01, Gaussian Inc., Wallingford, CT, 2004.

[11] A. Frisch, A.B. Nielson, A.J. Holder, GAUSSVIEW User Manual, Gaussian Inc., Wallingford, CT, 2003.

[12] A.D. Becke, J. Chem. Phys. 98 (1993) 5648–5652.

[13] A.W. Bauer, W.M.M. Kirby, J.C. Sherries, M. Truck, Am. J. Cl in. Pathol. 45 (1996) 493.

[14] A.H. Collins (Ed.), Microbiology Method, second ed., Butterworth, London, 1976.

[15] R. Cruickshank, J.P. Duguid, B.P. Marmion, R.H.A. Awain, Medicinal Microbiology, 12th ed., 11, Churchill Livingstone, London, 1995, p. 196.

[16] Blois, M.S., 1958. Antioxidant determinations by the use of a stable free radical. Nature. 29:1199-1200.

[17] I. Fleming, Frontier Orbitals and Organic Chemical Reactions, Wiley, London, 1976.

[18] T.A. Koopmans, Physica **1**, 104 (1993)

[19] H. Chermette, J. Comput. Chem. **20**, 129 (1999).

[20] R.G. Parr, L.V. Szentpaly and S. Liu, J. Am. Chem. Soc. **121**, 1922 (1999).

[21] S. AnieRoshan, C. Joseph, M.A. Ittyachen, Matter. Lett. **49**, 299 (2001).

[22] V.Venkataramanan, S. Maheswaran, J.N. Sherwood, H.L. Bhat, J. Cryst. Growth **173**(3-4), 605 (1997).

[23] A.K. Chawla, D. Kaur, R. Chandra, Optical Mater,
     29, 33 (2007).
[24] M.Dongol, Egypt, J. Solids **25**, 33 (2002).
[25] B.L. Zhu, C.S. Xie, D.W. Zeng, W.L. Song,
     A.H. Wang, Mater. Chem. Phys. **89**, 148 (2005).
[26] P.W. Zukowski, S.B. Kantorow, D. Maczka, V.F.
     Stelmakh, Phys. Stat. Sol. A **112**, 695 (1989).
[27] U. Von Hundelshausen, Phys. Lett. **34A**, 7 (1971).
[28] C. Balarew, R. Duhlew, J. Solid Sate Chem.
     55, 1 (1984).
[29] K.K. Bamzai, P.N. Kotru, B.M. Wanklyn, Appl. Surf.
     Sci. **133**, 195 (1998).
[30] E.M. Onitsch, Microscopia **2**, 131 (1947).
[31] M. Hanneman, Metall. Manch **23**, 135 (1941).
[32] W.A. Wooster, Rep. Prog. Phys. **16**, 62 (1953).

[33] Y.X. Sun, Q.L. Hao, W.X. Wei, Z.X. Yu, L.D. Lu,
     X.Wang, Y.S. Wang, J. Mol. Struct.: Theochem.
     904, 74 (2009).
[34] M. Sheik-Bahae, A. A. Said, Van E. W. Stryland,
     Opt. Let. **14**, 955 (1989).
[35] M. Sheik-Bahae, A.A. Said, T.H. Wei, D.J. Hagan,
     E.W. Van Stryland, IEEE J. Quantum Electron.
     26, 760 (1990).
[36] EsmaeilShshrisri and W. Mahmood, Am. J. Engg. and
     Applied Sci. **3**, 98 (2010).
[37] R. Ashok Kumar, R. EzhilVizhi, N. Vijayan,
     G. Bhagavannarayana and D. RajanBabu, J. Pure
     Appl. & Ind. Phys. **1**(1), 61 (2010).

_____

[*]Corresponding author: rbkrys@gmail.com